

Received: 13 July 2015 – Accepted: 13 August 2015 – Published: 31 August 2015

Correspondence to: Y. L. Sun (sunyele@mail.iap.ac.cn)

Published by Copernicus Publications on behalf of the European Geosciences Union.

ACPD

15, 23407–23455, 2015

**Aerosol composition,
oxidative properties,
and sources in
Beijing**

W. Q. Xu et al.

Title Page

Abstract

Introduction

Conclusions

References

Tables

Figures



Back

Close

Full Screen / Esc

Printer-friendly Version

Interactive Discussion



Abstract

The mitigation of air pollution in megacities remains a great challenge because of the complex sources and formation mechanisms of aerosol particles. The 2014 Asia-Pacific Economic Cooperation (APEC) summit in Beijing serves as a unique experiment to study the impacts of emission controls on aerosol composition, size distributions, and oxidative properties. Herein, a high-resolution time-of-flight aerosol mass spectrometer was deployed in urban Beijing for real-time measurements of size-resolved non-refractory submicron aerosol (NR-PM₁) species from 14 October to 12 November 2014, along with a range of collocated measurements. The average ($\pm\sigma$) PM₁ was 41.6 (± 38.9) $\mu\text{g m}^{-3}$ during APEC, which was decreased by 53% compared with that before APEC. The aerosol composition showed substantial changes owing to emission controls during APEC. Secondary inorganic aerosols (SIA = sulfate + nitrate + ammonium) showed significant reductions of 62–69%, whereas organics presented much smaller decreases (35%). The results from the positive matrix factorization of organic aerosols (OA) indicated that highly oxidized secondary OA (SOA) showed decreases similar to those of SIA during APEC. However, primary OA (POA) from cooking, traffic, and biomass burning sources were comparable to those before APEC, indicating the presence of strong local source emissions. The oxidation properties showed corresponding changes in response to OA composition. The average oxygen-to-carbon level during APEC was 0.36 (± 0.10), which is lower than the 0.43 (± 0.13) measured before APEC, demonstrating a decrease in the OA oxidation degree. The changes in size distributions of primary and secondary species varied during APEC. SIA and SOA showed significant reductions in large accumulation modes with peak diameters shifting from ~ 650 to 400 nm during APEC, whereas those of POA remained relatively unchanged. The changes in aerosol composition, size distributions, and oxidation degrees during the aging processes were further illustrated in a case study of a severe haze episode. Our results elucidated a complex response of aerosol chemistry to emission controls, which has significant implications that emission controls over regional scales can sub-

Aerosol composition, oxidative properties, and sources in Beijing

W. Q. Xu et al.

Title Page

Abstract

Introduction

Conclusions

References

Tables

Figures



Back

Close

Full Screen / Esc

Printer-friendly Version

Interactive Discussion



stantially reduce secondary particulates. However, stricter emission controls for local source emissions are needed for further mitigating air pollution in the megacity of Beijing.

1 Introduction

5 Atmospheric aerosols, especially fine particles of particulate matter (PM) with aerodynamic diameters less than $2.5\ \mu\text{m}$, play significant roles in human health hazards (Pope et al., 2009) and visibility reduction (Chow et al., 2002). Atmospheric aerosols also exert highly uncertain effects on climate change (Forster et al., 2007). Recently, the frequency of severe haze pollution events, which is characterized by high concentrations of fine particles, has become a significant concern in China (Zhang et al., 2010).
10 Consequently, extensive studies have been conducted to investigate the sources, formation mechanisms, and evolution processes of haze pollution during the last decade. The results showed that fine particles were mainly composed of organic matter (OM) and secondary inorganic aerosols (SIA) including sulfate, nitrate, and ammonium. The major sources of $\text{PM}_{2.5}$ were also identified and quantified by using receptor models, e.g., factor analysis, chemical mass balance, positive matrix factorization (PMF) (Zheng et al., 2005; Song et al., 2006; Wang et al., 2008; Zhang et al., 2013), and tracer-based methods (Dan et al., 2004; Cao et al., 2005; Guo et al., 2012). Overall, traffic exhaust, industrial emissions, coal combustion, biomass burning, and secondary aerosols were the major sources of $\text{PM}_{2.5}$.
15 Cooking aerosols (COA) were also found to be a significant contributor of $\text{PM}_{2.5}$ in urban environments (Huang, X.-F. et al., 2010; Sun et al., 2010, 2013). Recent studies further highlighted the important roles of SIA and secondary organic aerosols (SOA) in the formation of severe haze pollution (Sun et al., 2014; Huang et al., 2014; Zheng et al., 2015). The substantial emissions from
20 primary sources and rapid secondary aerosol formation coupled with stagnant meteorological conditions lead to frequent haze pollution in China, particularly during winter (Sun et al., 2014). However, because most previous studies are based on filter mea-

Aerosol composition, oxidative properties, and sources in Beijing

W. Q. Xu et al.

Title Page

Abstract

Introduction

Conclusions

References

Tables

Figures



Back

Close

Full Screen / Esc

Printer-friendly Version

Interactive Discussion



ments in the trailer included particle extinction (630 nm) of $PM_{2.5}$ by a cavity attenuated phase shift extinction monitor (CAPS PM_{ext} , Aerodyne Research Inc.), gaseous NO_2 by a CAPS- NO_2 , and black carbon (BC) by a two-wavelength aethalometer (model AE22, Magee Scientific Corp.). In addition, gaseous species (such as CO, O_3 , NO, NO_y and SO_2) were simultaneously measured at a nearby two-story building by using a series of gas analyzers from Thermo Scientific. Meteorological parameters such as relative humidity (RH), temperature, wind speed (WS), and wind direction (WD) were obtained at 15 elevations at the Beijing 325 m Meteorological Tower, which is approximately 30 m from the sampling site. All of the data in this study are reported in Beijing Standard Time (BST), which is equivalent to Coordinated Universal Time (UTC) plus 8 h.

2.1.2 HR-AMS operations

The HR-AMS was operated by alternating the mass-sensitive V-mode and the high-mass-resolution optical mode every 5 min. Under V-mode operation, the HR-AMS cycled through the mass spectrum (MS) and particle time-of-flight (PToF) modes every 10 s. No PToF data were collected in the W-mode due to the limited signal-to-noise (S/N) ratio. The particle-free ambient air was sampled and analyzed to determine the detection limits (DLs) of NR- PM_1 species and the fragment ion ratios of gases for subsequent high-resolution analysis. The 5 min DLs of organics, sulfate, nitrate, ammonium, and chloride of V and W-modes determined as three times the standard deviations (3σ) were 0.017, 0.010, 0.0016, 0.0014, and $0.004 \mu g m^{-3}$ and 0.030, 0.035, 0.026, 0.0049, and $0.032 \mu g m^{-3}$, respectively, which are close to the values reported in previous HR-AMS studies (DeCarlo et al., 2006). Prior to this study, the ionization efficiency (IE) and particle sizes were calibrated by using pure ammonium nitrate particles and polystyrene latex spheres (PSL, density = $1.05 g cm^{-3}$), respectively, following previous standard protocols (Jayne et al., 2000; Jimenez, 2003; Drewnick et al., 2005).

Aerosol composition, oxidative properties, and sources in Beijing

W. Q. Xu et al.

Title Page

Abstract

Introduction

Conclusions

References

Tables

Figures



Back

Close

Full Screen / Esc

Printer-friendly Version

Interactive Discussion



2.2 HR-AMS data analysis

The mass concentrations and size distributions of NR-PM₁ were analyzed by using standard AMS data analysis software (SQUIRREL v1.56 and PIKA v 1.15D) written in Igor Pro 6.12A (Wavemetrics, Lake Oswego, Ore., USA). A constant collection efficiency (CE) of 0.5 was applied for the quantification of NR-PM₁ species because the aerosol particles were dry and were slightly acidic as indicated by $\text{NH}_4^+_{\text{measured}}/\text{NH}_4^+_{\text{predicted}}$ (= 0.75) (Zhang et al., 2007). In addition, the overall mass fractions of ammonium nitrate were below the threshold value (40 %) that significantly affects the CE (Matthew et al., 2008). Therefore, the three major factors, humidity, particle acidity, and ammonium nitrate fraction, did not significantly affect the universal CE = 0.5, which has been widely used in numerous AMS studies. However, a constant CE value may introduce an uncertainty of 20–30 % for the mass concentrations of NR-PM₁ species (Middlebrook et al., 2012). The default relative ionization efficiencies (RIEs) of 1.4 for organics, 1.2 for sulfate, 1.1 for nitrate, and 1.3 for chloride were used (Allan et al., 2003) in this study; that for ammonium, 5.0, was determined from pure NH₄NO₃ particles. The total PM₁ mass (= NR-PM₁ + BC) agreed well with PM_{2.5} ($R^2 = 0.86$). The average ratio of PM₁/PM_{2.5}, 0.77, was also consistent with that reported in previous studies (Sun et al., 2014). This result further supports that CE = 0.5 is reasonable for this study.

The high-resolution mass spectra (HRMS) of the V- and W-modes were analyzed for ion-speciated fragments of C_xH_y⁺, C_xH_yO_z⁺, C_xH_yN_p⁺, and C_xH_yO_zN_p⁺ by using PIKA v1.15D. The elemental composition of OA, including ratios of oxygen-to-carbon (O/C), hydrogen-to-carbon (H/C), organic mass to organic carbon (OM/OC), and nitrogen-to-carbon (N/C), were determined by using the elemental analysis approach recommended by Aiken et al. (2007), referred to as A-A. We also calculated the elemental ratios by using the improved calibration factors recommended by Canagaratna et al. (2015), referred to as I-A. The average A-A H/C and O/C ratios were 1.55 and 0.41, which are respectively 8 and 20 % lower than the I-A H/C and O/C ra-

Title Page

Abstract

Introduction

Conclusions

References

Tables

Figures

◀

▶

◀

▶

Back

Close

Full Screen / Esc

Printer-friendly Version

Interactive Discussion



tios of 1.69 and 0.51. For consistency with previous studies, the elemental composition determined by using the A-A approach in this study. In addition, the oxidation state ($\overline{OS} = 2 \times O/C - H/C$) (Kroll et al., 2011) of OA was calculated to be -0.73 and -0.67 with the A-A and I-A methods, respectively.

The PMF2.exe algorithm (v4.2) in robust mode (Paatero and Tapper, 1994) was applied to the HRMS of OA to resolve distinct OA factors representing specific sources and processes. Values of m/z larger than 120 were excluded due to the limited mass resolution in separating higher mass ions. Isotopic ions scaled on the basis of the signals of parent ions were also excluded. Such exclusion had a minor impact on the total mass ($\sim 2-3\%$). Other data-pretreatments were similar to those reported in previous studies; that is, bad ions with $S/N < 0.2$ were removed, and the “weak” ions with $0.2 < S/N < 3$ were further down-weighted by increasing their errors by a factor of three.

The PMF solutions were investigated in detail by evaluating the mass spectral profiles and time series of OA factors (1 to 10) as a function of rotational parameter (fPeak). By comparing the mass spectral profiles of OA factors with previously reported standard mass spectra, and the time series with external tracers, such as CO, NO_x , BC, SIA, $C_3H_5O^+$, and $C_2H_3O^+$, a six-factor solution with fPeak = 0 was selected in this work. Although the SOA was a mixed factor for the five-factor solution, the seven-factor solution split the SV-OOA into two components, which cannot be reasonably explained due to limited external tracers. Summary of the key diagnostic plots of the PMF results are shown in Figs. S1–S3 in the Supplement.

3 Results and discussion

3.1 Mass concentrations and chemical composition

Figure 1 shows the time series of submicron aerosol species during the entire study period. All aerosol species varied dramatically between haze episodes and clean peri-

Aerosol composition, oxidative properties, and sources in Beijing

W. Q. Xu et al.

Title Page

Abstract

Introduction

Conclusions

References

Tables

Figures

◀

▶

◀

▶

Back

Close

Full Screen / Esc

Printer-friendly Version

Interactive Discussion



**Aerosol composition,
oxidative properties,
and sources in
Beijing**

W. Q. Xu et al.

[Title Page](#)[Abstract](#)[Introduction](#)[Conclusions](#)[References](#)[Tables](#)[Figures](#)[◀](#)[▶](#)[◀](#)[▶](#)[Back](#)[Close](#)[Full Screen / Esc](#)[Printer-friendly Version](#)[Interactive Discussion](#)

ods. As indicated in the figure, three evident pollution episodes and two episodes were observed before and during APEC, respectively. The formation and evolution of the haze episodes were closely related to stagnant meteorology characterized by low WS and high RH. The average ($\pm\sigma$) mass concentration of PM_{10} was $41.6 (\pm 38.9) \mu\text{g m}^{-3}$ during APEC, which was 52.7 % lower than the $88.0 \mu\text{g m}^{-3}$ measured before APEC. Periods of high PM_{10} concentration ($> 60 \mu\text{g m}^{-3}$) accounted for 56.7 % of the time before APEC and 22.6 % during APEC. These results indicate significant reductions in PM during APEC, particularly for pollution events with high PM_{10} loading.

The variations of inorganic aerosol and organics showed different behaviors before and during APEC. Figure 1c shows clear decreases in inorganic aerosol species on 3 November, when emission controls were first implemented in Beijing. Relatively low ambient levels were maintained on 6 November, when far stricter emission controls were imposed in Beijing and in the surrounding regions. As a comparison, the variations in organics were more dramatic, and the changes during APEC were not as significant as those for inorganic aerosol species. Although SIAs such as sulfate, nitrate, and ammonium were decreased by 62–69 % during APEC, organics showed a much smaller decrease of 35 % (Table 1). The chemical composition of PM_{10} before APEC was mainly organics, accounting for 38.0 %, followed by nitrate at 26.4 % and sulfate at 13.7 %. The average aerosol composition during APEC showed significant changes. Organics showed a large increase, accounting for more than half of PM_{10} , whereas the contribution of SIA was decreased from 51.2 to 35.4 %. These results suggest different responses of SIA and OA to emission controls. Compared with that reported in previous studies in Beijing, we observed a significantly higher nitrate contribution before APEC in summer 2008 (15.8 %) (Huang, X.-F. et al., 2010) and in winter 2011–2012 (16.0 %) (Sun et al., 2013). The average mass ratio of NO_3/SO_4 was 1.78, which is also significantly higher than the values previously reported in China (Zhang, Y. M. et al., 2014). Thus, our results elucidate the important role of nitrate in PM pollution during the study period.

consistent with the diurnal variations of diesel trucks and heavy-duty vehicles that are only allowed to operate inside the city between 22:00–6:00. Different from other aerosol species, the reduction in BC was relatively constant at 47.0–67.5 % throughout the day, suggesting similar BC sources before and during APEC, but with different emission intensities. In addition, the mountain-valley breeze effect on BC was different from that on other species, likely due to the similar BC levels in northwest and south Beijing.

3.3 Composition and sources of OA

Six OA factors were identified by PMF analysis of HRMS of OA, including four primary OA factors (HOA, BBOA, COA1, and COA2), and two secondary OA factors (SV-OOA and LV-OOA). The mass spectra and time series of the six OA factors are shown in Fig. 5.

The HOA spectrum was characterized by prominent hydrocarbon ion series of $C_nH_{2n+1}^+$ and $C_nH_{2n-1}^+$, which is consistent with that observed at various urban sites (Huang, X.-F. et al., 2010; Sun et al., 2011; Xu et al., 2014). The O/C ratio of HOA was 0.17, which is considerably higher than 0.03–0.04 measured from diesel and gasoline exhausts (Mohr et al., 2009) and slightly higher than 0.11–0.13 observed in the YRD (Huang et al., 2013), and the PRD in China (He et al., 2011), indicating that the HOA in this study was relatively oxidized. HOA correlated well with BC ($R^2 = 0.78$) during APEC, and the average HOA/BC ratio of 1.2 was consistent with that obtained in other megacities such as Mexico City (Aiken et al., 2009) and New York City (Sun et al., 2011). Although HOA also tightly correlated with BC before APEC ($R^2 = 0.66$), a significantly lower ratio of HOA/BC (0.57) was observed. These results suggest a substantial change of the sources of either HOA or BC during APEC. As shown in Fig. 3, BC showed large reductions similar to those of SIA during APEC, suggesting that a large fraction of BC was likely from regional transport. This result is consistent with a recent study (Xu et al., 2014) in which 53 % of BC was found to be associated with SIA and SOA at an urban site in Lanzhou, and the rest 47 % was from local primary emissions. Therefore, we infer that the HOA/BC ratio of 1.2 during APEC is likely representative

Aerosol composition, oxidative properties, and sources in Beijing

W. Q. Xu et al.

Title Page

Abstract

Introduction

Conclusions

References

Tables

Figures



Back

Close

Full Screen / Esc

Printer-friendly Version

Interactive Discussion



**Aerosol composition,
oxidative properties,
and sources in
Beijing**

W. Q. Xu et al.

Title Page

Abstract

Introduction

Conclusions

References

Tables

Figures

◀

▶

◀

▶

Back

Close

Full Screen / Esc

Printer-friendly Version

Interactive Discussion



et al., 2011) ($R^2 = 0.96$) than COA2 ($R^2 = 0.81$ – 0.83), which is indicative of their different sources. The diurnal cycles of COA1 and COA2 were both characterized by pronounced evening peaks with maximum concentrations occurring between 20:00 and 21:00, indicating the large amount of cooking activities at nighttime. Note that the diurnal cycle of COA1 showed clear morning and noon peaks associated with breakfast and lunch emissions, which were almost invisible for COA2. Interestingly, a significant decrease in COA1 concentration was not observed during APEC, suggesting similar local cooking sources near the sampling site before and during APEC. However, COA2 showed a considerable reduction from late afternoon to mid-night during APEC. This result suggests that the sources of COA2 were controlled by a certain degree during APEC. Considering that the major control of cooking emissions was the banning of open charcoal grills, we conclude that the COA2 was primarily from charbroiling emissions, whereas COA1 was more like a factor of regular cooking emissions.

The BBOA spectrum showed pronounced peaks at m/z 60, mainly $C_2H_4O_2^+$, and m/z 73, mainly $C_3H_5O_2^+$; these two marker ions indicate the presence of biomass burning (Alfarra et al., 2007; Aiken et al., 2009; Cubison et al., 2011). BBOA correlated strongly with $C_2H_4O_2^+$ before and during APEC ($R^2 = 0.65$ and 0.88 , respectively). The weaker correlation before APEC is likely due to other source contributions to $C_2H_4O_2^+$ such as cooking aerosol (COA2). The O/C ratio of BBOA was 0.50, which is significantly higher than that observed in Kaiping and Jiaying in China at 0.26–0.27 (Huang et al., 2011, 2013), and in Mexico City at 0.30 (Aiken et al., 2009). The f_{44} of BBOA, at 11.3% was higher as well. Because biomass burning, e.g., agricultural burning in October, was rare inside the city of Beijing, the observed BBOA was expected to be mainly from regional transport. Previous studies have shown that BBOA can be rapidly oxidized in the atmosphere, leading to a decrease in f_{60} and a corresponding increase in f_{44} (Cubison et al., 2011). Therefore, we infer that BBOA in this study was an aged BBOA from regional transport. In fact, the O/C ratio of BBOA was close to that of the aged BBOA observed from the aircraft measurements during the Megacity Initiative: Local and Global Research Observations (MILAGRO) project in 2006 (DeCarlo

indicates their slightly different aging processes mainly driven by the additions of carboxylic acid with fragmentation (Ng et al., 2011). The slope in this study is less than that measured in Changdao at -0.63 (Hu et al., 2013), Shenzhen at -0.87 (He et al., 2011), and Kaiping in PRD at -0.76 (Huang et al., 2011), indicating that the aging mechanism of OA varies among different sites and seasons in China.

As shown in Fig. 12a, The O/C varied dramatically and showed no clear dependence on RH at low RH levels of $< 60\%$, although a positive increase as a function of RH before APEC was observed at $\text{RH} > 60\%$. These results might indicate that aqueous-phase processing at high RH levels increased the oxidation degree of OA. The POA with high concentration at nighttime when RH is correspondingly high can have a large influence on the O/C of total OA, which explains the slight decrease in O/C as a function of RH during APEC. The O/C ratio of SOA was calculated, and its relationship with RH is shown in Fig. 12b. It is clear that the O/C ratio of SOA rapidly increased from 0.5 to 0.8 as the RH increased from 10 to $> 80\%$ before APEC. The O/C of SOA showed similar RH dependence during APEC. Such an increase is mainly caused by a faster increase of LV-OOA than that of SV-OOA. These results likely indicate that aqueous-phase processing produced highly aged OA during the severe haze pollution episodes. However, we found that LV-OOA tightly correlated with NO_3 ($R^2 = 0.94$), whereas aqueous-phase production appeared to play an insignificant role in nitrate formation during winter (Sun et al., 2013). Therefore, the highly aged OA at high RH levels was more likely due to the aging of LV-OOA for a longer time during the transport to Beijing. Further studies are needed to investigate the role of aqueous-phase processing in the alteration of the oxidation properties of OA.

3.6 Case study of the evolution of a severe haze episode

The four-day evolution of a severe pollution episode was observed between 22 and 25 October during which the average PM_{10} concentration showed a 10 fold increase from < 30 to $> 300 \mu\text{g m}^{-3}$. As shown in Fig. 13, this evolution period was characterized by prevailing southerly winds and air masses (Fig. S5), low WS ($< 4 \text{ m s}^{-1}$) across the

67% of the total OA, which together contributed 82% of the total PM₁, further elucidating the significant role of secondary aerosol in haze formation.

Although SIA was observed to gradually increase during the evolution of this haze episode, primary aerosol species such as COA, HOA, and BC showed similar diurnal variations during S3 and S4, indicating relatively constant local emissions during these two stages. Although the daily maximum of O/C showed a continuous increase, pronounced diurnal cycles with the lowest values occurring at mid-night were also observed due to the influences of local primary OA. The O/C of SOA was then calculated for a better illustration of OA aging. As shown in Fig. 13d, the O/C ratio of SOA showed a gradual increase from ~ 0.55 to 0.8 during S1–S3 and remained consistently high (~ 0.8) during S4. This result is consistent with the relative contributions of LV-OOA and SV-OOA during the four evolution stages. Although SV-OOA was higher than LV-OOA during S1, LV-OOA gradually exceeded SV-OOA and became the dominant contributor of OA during the following three stages. These results illustrate that the aging of the haze episode was associated with significant formation of highly oxidized OA. The Van Krevelen diagram of H/C versus O/C for this haze episode is shown in Fig. 11. It is clear that OA evolved rapidly during this haze episode, showing an increase in O/C associated with a corresponding decrease in H/C with a slope of -0.6.

Figure 14 shows the evolution of size distributions of sulfate, nitrate, and organics during this haze episode. Sulfate and nitrate showed evident particle growth as a function of time. Although broad size distributions peaking at ~ 350 nm were observed during S1, the peak diameters gradually evolved to ~ 700 nm during S4; these size distributions were characterized by single large accumulation modes. Organics showed similar size evolution behavior as that of sulfate and nitrate but presented significant contributions from particles smaller than 200 nm. In particular, the influences of local primary emissions such as cooking and traffic on small particles were observed at nighttime during 23–25 October. Overall, the aerosol composition, oxidative properties, and size distributions exhibited substantial changes during the evolution of the

Aerosol composition, oxidative properties, and sources in Beijing

W. Q. Xu et al.

Title Page

Abstract

Introduction

Conclusions

References

Tables

Figures



Back

Close

Full Screen / Esc

Printer-friendly Version

Interactive Discussion



severe haze episode, which was characterized by the significant enhancement of SIA and SOA with high oxidation degrees and large particle diameters.

4 Conclusions

China imposed strict emission controls in Beijing and its surrounding regions during the 2014 APEC summit. In this study, we present a detailed investigation of the impacts of emission controls on the changes in chemical composition, oxidative properties, and size distributions of submicron aerosols. The average mass concentration of PM₁ showed a substantial decrease from 88.0 μg m⁻³ before APEC to 41.6 μg m⁻³ during APEC. The aerosol composition also showed significant changes. Although submicron aerosols were composed mainly of organics, at 38.0%, followed by nitrate at 26.4% and sulfate at 13.7% before APEC, the contribution of organics was observed to have a significant increase at 52.4% associated with the significant reductions of SIA during APEC. This result demonstrates the different responses of SIA and OA to regional emission controls. PMF analysis of OA identified three primary sources such as traffic, cooking, and biomass burning emissions and two secondary factors with different oxidation degrees. The highly oxidized LV-OOA showed reductions similar to those of SIA with the contribution to OA decreasing from 30 to 14%. In contrast, POA showed elevated contributions indicating the presence of strong local source emissions during APEC. The O/C ratio of OA decreased from 0.43 to 0.36, demonstrating a decrease in the oxidation degree of OA during APEC. The peak diameters in size distributions of SIA and SOA were ~ 650 nm before APEC and shifted to smaller sizes of ~ 400 nm during APEC. This result illustrates that emission controls of secondary aerosol precursors exerted a dominant impact in reducing accumulation mode particles. Comparatively, the size distributions of POA remained relatively unchanged. Therefore, our results elucidated significant changes in chemical composition, size distributions, and oxidative properties of aerosol particles as a result of emission controls. In addition, we observed significant changes in aerosol properties during the aging processes of a se-

23432

ACPD

15, 23407–23455, 2015

Aerosol composition, oxidative properties, and sources in Beijing

W. Q. Xu et al.

Title Page

Abstract

Introduction

Conclusions

References

Tables

Figures

◀

▶

◀

▶

Back

Close

Full Screen / Esc

Printer-friendly Version

Interactive Discussion



**Aerosol composition,
oxidative properties,
and sources in
Beijing**

W. Q. Xu et al.

Title Page

Abstract

Introduction

Conclusions

References

Tables

Figures



Back

Close

Full Screen / Esc

Printer-friendly Version

Interactive Discussion



sources and processing of organic aerosol over the Central Mexican Plateau from aircraft measurements during MILAGRO, *Atmos. Chem. Phys.*, 10, 5257–5280, doi:10.5194/acp-10-5257-2010, 2010.

5 Drewnick, F., Hings, S. S., DeCarlo, P., Jayne, J. T., Gonin, M., Fuhrer, K., Weimer, S., Jimenez, J. L., Demerjian, K. L., Borrmann, S., and Worsnop, D. R.: A New Time-of-Flight Aerosol Mass Spectrometer (TOF-AMS) – instrument description and first field deployment, *Aerosol Sci. Tech.*, 39, 637–658, doi:10.1080/02786820500182040, 2005.

10 Forster, P., Ramaswamy, V., Artaxo, P., Bernsten, T., Betts, R., Fahey, D. W., Haywood, J., Lean, J., Lowe, D. C., Myhre, G., Nganga, J., Prinn, R., Raga, G., Schulz, M., and Dorland, R. V.: Changes in atmospheric constituents and in radiative forcing, in: *Climate Change 2007: The Physical Science Basis. Contribution of Working Group I to the Fourth Assessment Report of the Intergovernmental Panel on Climate Change*, edited by: Solomon, S., Qin, D., Manning, M., Chen, Z., Marquis, M., Averyt, K. B., Tignor, M., and Miller, H. L., Cambridge University Press, Cambridge, UK and New York, NY, USA, 153–171, 2007.

15 Ge, X., Setyan, A., Sun, Y., and Zhang, Q.: Primary and secondary organic aerosols in Fresno, California during wintertime: results from high resolution aerosol mass spectrometry, *J. Geophys. Res.*, 117, D19301, doi:10.1029/2012JD018026, 2012a.

20 Ge, X., Zhang, Q., Sun, Y., Ruehl, C. R., and Setyan, A.: Effect of aqueous-phase processing on aerosol chemistry and size distributions in Fresno, California, during wintertime, *Environ. Chem.*, 9, 221, doi:10.1071/en11168, 2012b.

Guo, S., Hu, M., Guo, Q., Zhang, X., Zheng, M., Zheng, J., Chang, C.-C., Schauer, J. J., and Zhang, R.: Primary sources and secondary formation of organic aerosols in Beijing, China, *Environ. Sci. Technol.*, doi:10.1021/es2042564, 2012.

25 Guo, S., Hu, M., Guo, Q., Zhang, X., Schauer, J. J., and Zhang, R.: Quantitative evaluation of emission controls on primary and secondary organic aerosol sources during Beijing 2008 Olympics, *Atmos. Chem. Phys.*, 13, 8303–8314, doi:10.5194/acp-13-8303-2013, 2013.

Han, S., Kondo, Y., Oshima, N., Takegawa, N., Miyazaki, Y., Hu, M., Lin, P., Deng, Z., Zhao, Y., Sugimoto, N., and Wu, Y.: Temporal variations of elemental carbon in Beijing, *J. Geophys. Res.*, 114, D23202, doi:10.1029/2009jd012027, 2009.

30 He, L.-Y., Lin, Y., Huang, X.-F., Guo, S., Xue, L., Su, Q., Hu, M., Luan, S.-J., and Zhang, Y.-H.: Characterization of high-resolution aerosol mass spectra of primary organic aerosol emissions from Chinese cooking and biomass burning, *Atmos. Chem. Phys.*, 10, 11535–11543, doi:10.5194/acp-10-11535-2010, 2010.

**Aerosol composition,
oxidative properties,
and sources in
Beijing**

W. Q. Xu et al.

[Title Page](#)[Abstract](#)[Introduction](#)[Conclusions](#)[References](#)[Tables](#)[Figures](#)[Back](#)[Close](#)[Full Screen / Esc](#)[Printer-friendly Version](#)[Interactive Discussion](#)

He, L.-Y., Huang, X.-F., Xue, L., Hu, M., Lin, Y., Zheng, J., Zhang, R., and Zhang, Y.-H.: Submicron aerosol analysis and organic source apportionment in an urban atmosphere in Pearl River Delta of China using high-resolution aerosol mass spectrometry, *J. Geophys. Res.*, 116, D12304, doi:10.1029/2010jd014566, 2011.

5 Heald, C. L., Kroll, J. H., Jimenez, J. L., Docherty, K. S., DeCarlo, P. F., Aiken, A. C., Chen, Q., Martin, S. T., Farmer, D. K., and Artaxo, P.: A simplified description of the evolution of organic aerosol composition in the atmosphere, *Geophys. Res. Lett.*, 37, L08803, doi:10.1029/2010gl042737, 2010.

10 Hu, W. W., Hu, M., Yuan, B., Jimenez, J. L., Tang, Q., Peng, J. F., Hu, W., Shao, M., Wang, M., Zeng, L. M., Wu, Y. S., Gong, Z. H., Huang, X. F., and He, L. Y.: Insights on organic aerosol aging and the influence of coal combustion at a regional receptor site of central eastern China, *Atmos. Chem. Phys.*, 13, 10095–10112, doi:10.5194/acp-13-10095-2013, 2013.

15 Huang, R. J., Zhang, Y., Bozzetti, C., Ho, K. F., Cao, J. J., Han, Y., Daellenbach, K. R., Slowik, J. G., Platt, S. M., Canonaco, F., Zotter, P., Wolf, R., Pieber, S. M., Brunts, E. A., Crippa, M., Ciarelli, G., Piazzalunga, A., Schwikowski, M., Abbaszade, G., Schnelle-Kreis, J., Zimmermann, R., An, Z., Szidat, S., Baltensperger, U., El Haddad, I., and Prevot, A. S.: High secondary aerosol contribution to particulate pollution during haze events in China, *Nature*, 514, 218–222, doi:10.1038/nature13774, 2014.

20 Huang, X., Xue, L., He, L., Hu, M., Zhang, Y., and Zhu, T.: On-line measurement of organic aerosol elemental composition based on high resolution aerosol mass spectrometry, *Chin. Sci. Bull.*, 55, 3391–3396, doi:10.1360/032012-384, 2010.

25 Huang, X.-F., He, L.-Y., Hu, M., Canagaratna, M. R., Sun, Y., Zhang, Q., Zhu, T., Xue, L., Zeng, L.-W., Liu, X.-G., Zhang, Y.-H., Jayne, J. T., Ng, N. L., and Worsnop, D. R.: Highly time-resolved chemical characterization of atmospheric submicron particles during 2008 Beijing Olympic Games using an Aerodyne High-Resolution Aerosol Mass Spectrometer, *Atmos. Chem. Phys.*, 10, 8933–8945, doi:10.5194/acp-10-8933-2010, 2010.

30 Huang, X.-F., He, L.-Y., Hu, M., Canagaratna, M. R., Kroll, J. H., Ng, N. L., Zhang, Y.-H., Lin, Y., Xue, L., Sun, T.-L., Liu, X.-G., Shao, M., Jayne, J. T., and Worsnop, D. R.: Characterization of submicron aerosols at a rural site in Pearl River Delta of China using an Aerodyne High-Resolution Aerosol Mass Spectrometer, *Atmos. Chem. Phys.*, 11, 1865–1877, doi:10.5194/acp-11-1865-2011, 2011.

**Aerosol composition,
oxidative properties,
and sources in
Beijing**

W. Q. Xu et al.

Title Page

Abstract

Introduction

Conclusions

References

Tables

Figures



Back

Close

Full Screen / Esc

Printer-friendly Version

Interactive Discussion



Huang, X.-F., He, L.-Y., Xue, L., Sun, T.-L., Zeng, L.-W., Gong, Z.-H., Hu, M., and Zhu, T.: Highly time-resolved chemical characterization of atmospheric fine particles during 2010 Shanghai World Expo, *Atmos. Chem. Phys.*, 12, 4897–4907, doi:10.5194/acp-12-4897-2012, 2012.

Huang, X.-F., Xue, L., Tian, X.-D., Shao, W.-W., Sun, T.-L., Gong, Z.-H., Ju, W.-W., Jiang, B., Hu, M., and He, L.-Y.: Highly time-resolved carbonaceous aerosol characterization in Yangtze River Delta of China: composition, mixing state and secondary formation, *Atmos. Environ.*, 64, 200–207, doi:10.1016/j.atmosenv.2012.09.059, 2013.

Jayne, J. T., Leard, D. C., Zhang, X., Davidovits, P., Smith, K. A., Kolb, C. E., and Worsnop, D. R.: Development of an aerosol mass spectrometer for size and composition analysis of submicron particles, *Aerosol Sci. Tech.*, 33, 49–70, 2000.

Jimenez, J. L.: Ambient aerosol sampling using the Aerodyne Aerosol Mass Spectrometer, *J. Geophys. Res.*, 108, D7, doi:10.1029/2001jd001213, 2003.

Kroll, J. H., Donahue, N. M., Jimenez, J. L., Kessler, S. H., Canagaratna, M. R., Wilson, K. R., Altieri, K. E., Mazzoleni, L. R., Wozniak, A. S., Bluhm, H., Mysak, E. R., Smith, J. D., Kolb, C. E., and Worsnop, D. R.: Carbon oxidation state as a metric for describing the chemistry of atmospheric organic aerosol, *Nature Chem.*, 3, 133–139, doi:10.1038/nchem.948, 2011.

Lee, B. P., Li, Y. J., Yu, J. Z., Louie, P. K. K., and Chan, C. K.: Physical and chemical characterization of ambient aerosol by HR-ToF-AMS at a suburban site in Hong Kong during springtime 2011, *J. Geophys. Res.*, 118, 8625–8639, doi:10.1002/jgrd.50658, 2013.

Matthew, B. M., Middlebrook, A. M., and Onasch, T. B.: Collection efficiencies in an aerodyne aerosol mass spectrometer as a function of particle phase for laboratory generated aerosols, *Aerosol Sci. Tech.*, 42, 884–898, doi:10.1080/02786820802356797, 2008.

Middlebrook, A. M., Bahreini, R., Jimenez, J. L., and Canagaratna, M. R.: Evaluation of composition-dependent collection efficiencies for the aerodyne aerosol mass spectrometer using field data, *Aerosol Sci. Tech.*, 46, 258–271, doi:10.1080/02786826.2011.620041, 2012.

Mohr, C., Huffman, J. A., Cubison, M. J., Aiken, A. C., Docherty, K. S., Kimmel, J. R., Ulbrich, I. M., Hannigan, M., and Jimenez, J. L.: Characterization of primary organic aerosol emissions from meat cooking, trash burning, and motor vehicles with High-Resolution Aerosol Mass Spectrometry and comparison with ambient and chamber observations, *Environ. Sci. Technol.*, 43, 2443–2449, doi:10.1021/es8011518, 2009.

**Aerosol composition,
oxidative properties,
and sources in
Beijing**

W. Q. Xu et al.

Title Page

Abstract

Introduction

Conclusions

References

Tables

Figures



Back

Close

Full Screen / Esc

Printer-friendly Version

Interactive Discussion



- Ng, N. L., Canagaratna, M. R., Jimenez, J. L., Chhabra, P. S., Seinfeld, J. H., and Worsnop, D. R.: Changes in organic aerosol composition with aging inferred from aerosol mass spectra, *Atmos. Chem. Phys.*, 11, 6465–6474, doi:10.5194/acp-11-6465-2011, 2011.
- Paatero, P. and Tapper, U.: Positive matrix factorization: a non-negative factor model with optimal utilization of error estimates of data values, *Environmetrics*, 5, 111–126, 1994.
- Pope III, C. A., Ezzati, M., and Dockery, D. W.: Fine-particulate air pollution and life expectancy in the United States, *New Engl. J. Med.*, 360, 376–386, doi:10.1056/NEJMsa0805646, 2009.
- Shao, M., Wang, B., Lu, S., Yuan, B., and Wang, M.: Effects of Beijing Olympics control measures on reducing reactive hydrocarbon species, *Environ. Sci. Technol.*, 45, 514–519, doi:10.1021/es102357t, 2011.
- Song, Y., Zhang, Y., Xie, S., Zeng, L., Zheng, M., Salmon, L. G., Shao, M., and Slanina, S.: Source apportionment of PM_{2.5} in Beijing by positive matrix factorization, *Atmos. Environ.*, 40, 1526–1537, doi:10.1016/j.atmosenv.2005.10.039, 2006.
- Sun, J., Zhang, Q., Canagaratna, M. R., Zhang, Y., Ng, N. L., Sun, Y., Jayne, J. T., Zhang, X., Zhang, X., and Worsnop, D. R.: Highly time- and size-resolved characterization of submicron aerosol particles in Beijing using an Aerodyne Aerosol Mass Spectrometer, *Atmos. Environ.*, 44, 131–140, doi:10.1016/j.atmosenv.2009.03.020, 2010.
- Sun, Y., Wang, Z., Dong, H., Yang, T., Li, J., Pan, X., Chen, P., and Jayne, J. T.: Characterization of summer organic and inorganic aerosols in Beijing, China with an Aerosol Chemical Speciation Monitor, *Atmos. Environ.*, 51, 250–259, doi:10.1016/j.atmosenv.2012.01.013, 2012.
- Sun, Y., Jiang, Q., Wang, Z., Fu, P., Li, J., Yang, T., and Yin, Y.: Investigation of the sources and evolution processes of severe haze pollution in Beijing in January 2013, *J. Geophys. Res.-Atmos.*, 119, 4380–4398, doi:10.1002/2014jd021641, 2014.
- Sun, Y.-L., Zhang, Q., Schwab, J. J., Demerjian, K. L., Chen, W.-N., Bae, M.-S., Hung, H.-M., Hogrefe, O., Frank, B., Rattigan, O. V., and Lin, Y.-C.: Characterization of the sources and processes of organic and inorganic aerosols in New York city with a high-resolution time-of-flight aerosol mass spectrometer, *Atmos. Chem. Phys.*, 11, 1581–1602, doi:10.5194/acp-11-1581-2011, 2011.
- Sun, Y. L., Zhang, Q., Schwab, J. J., Chen, W.-N., Bae, M.-S., Hung, H.-M., Lin, Y.-C., Ng, N. L., Jayne, J., Massoli, P., Williams, L. R., and Demerjian, K. L.: Characterization of near-highway submicron aerosols in New York City with a high-resolution aerosol mass spectrometer, *Atmos. Chem. Phys.*, 12, 2215–2227, doi:10.5194/acp-12-2215-2012, 2012.

**Aerosol composition,
oxidative properties,
and sources in
Beijing**

W. Q. Xu et al.

Title Page

Abstract

Introduction

Conclusions

References

Tables

Figures



Back

Close

Full Screen / Esc

Printer-friendly Version

Interactive Discussion



Sun, Y. L., Wang, Z. F., Fu, P. Q., Yang, T., Jiang, Q., Dong, H. B., Li, J., and Jia, J. J.: Aerosol composition, sources and processes during wintertime in Beijing, China, *Atmos. Chem. Phys.*, 13, 4577–4592, doi:10.5194/acp-13-4577-2013, 2013.

Takegawa, N., Miyakawa, T., Watanabe, M., Kondo, Y., Miyazaki, Y., Han, S., Zhao, Y., van Pinxteren, D., Brüggemann, E., Gnauk, T., Herrmann, H., Xiao, R., Deng, Z., Hu, M., Zhu, T., and Zhang, Y.: Performance of an Aerodyne Aerosol Mass Spectrometer (AMS) during intensive campaigns in China in the Summer of 2006, *Aerosol Sci. Tech.*, 43, 189–204, doi:10.1080/02786820802582251, 2009.

Ulbrich, I. M., Canagaratna, M. R., Zhang, Q., Worsnop, D. R., and Jimenez, J. L.: Interpretation of organic components from Positive Matrix Factorization of aerosol mass spectrometric data, *Atmos. Chem. Phys.*, 9, 2891–2918, doi:10.5194/acp-9-2891-2009, 2009.

Wang, H., Zhuang, Y., Wang, Y., Sun, Y., Yuan, H., Zhuang, G., and Hao, Z.: Long-term monitoring and source apportionment of PM_{2.5}/PM₁₀ in Beijing, China, *J. Environ. Sci.*, 20, 1323–1327, 2008.

Wang, T., Nie, W., Gao, J., Xue, L. K., Gao, X. M., Wang, X. F., Qiu, J., Poon, C. N., Meinardi, S., Blake, D., Wang, S. L., Ding, A. J., Chai, F. H., Zhang, Q. Z., and Wang, W. X.: Air quality during the 2008 Beijing Olympics: secondary pollutants and regional impact, *Atmos. Chem. Phys.*, 10, 7603–7615, doi:10.5194/acp-10-7603-2010, 2010.

Wang, W., Primbs, T., Tao, S., and Simonich, S. L. M.: Atmospheric particulate matter pollution during the 2008 Beijing Olympics, *Environ. Sci. Technol.*, 43, 5314–5320, doi:10.1021/es9007504, 2009.

Wang, W., Jariyasopit, N., Schrlau, J., Jia, Y., Tao, S., Yu, T.-W., Dashwood, R. H., Zhang, W., Wang, X., and Simonich, S. L. M.: Concentration and photochemistry of PAHs, NPAHs, and OPAHs and toxicity of PM_{2.5} during the Beijing Olympic Games, *Environ. Sci. Technol.*, 45, 6887–6895, doi:10.1021/es201443z, 2011.

Xu, J., Zhang, Q., Chen, M., Ge, X., Ren, J., and Qin, D.: Chemical composition, sources, and processes of urban aerosols during summertime in northwest China: insights from high-resolution aerosol mass spectrometry, *Atmos. Chem. Phys.*, 14, 12593–12611, doi:10.5194/acp-14-12593-2014, 2014.

Zhang, J., Wang, Y., Huang, X., Liu, Z., Ji, D., and Sun, Y.: Characterization of organic aerosols in Beijing using an aerodyne high-resolution aerosol mass spectrometer, *Adv. Atmos. Sci.*, 32, 877–888, doi:10.1007/s00376-014-4153-9, 2015.

**Aerosol composition,
oxidative properties,
and sources in
Beijing**

W. Q. Xu et al.

Title Page

Abstract

Introduction

Conclusions

References

Tables

Figures

◀

▶

◀

▶

Back

Close

Full Screen / Esc

Printer-friendly Version

Interactive Discussion



- Zhang, J. K., Sun, Y., Liu, Z. R., Ji, D. S., Hu, B., Liu, Q., and Wang, Y. S.: Characterization of submicron aerosols during a month of serious pollution in Beijing, 2013, *Atmos. Chem. Phys.*, 14, 2887–2903, doi:10.5194/acp-14-2887-2014, 2014.
- Zhang, Q., Worsnop, D. R., Canagaratna, M. R., and Jimenez, J. L.: Hydrocarbon-like and oxygenated organic aerosols in Pittsburgh: insights into sources and processes of organic aerosols, *Atmos. Chem. Phys.*, 5, 3289–3311, doi:10.5194/acp-5-3289-2005, 2005.
- Zhang, Q., Jimenez, J. L., Worsnop, D. R., and Canagaratna, M.: A case study of urban particle acidity and its effect on secondary organic aerosol, *Environ. Sci. Technol.*, 41, 3213–3219, 2007.
- Zhang, Q. H., Zhang, J. P., and Xue, H. W.: The challenge of improving visibility in Beijing, *Atmos. Chem. Phys.*, 10, 7821–7827, doi:10.5194/acp-10-7821-2010, 2010.
- Zhang, R., Jing, J., Tao, J., Hsu, S.-C., Wang, G., Cao, J., Lee, C. S. L., Zhu, L., Chen, Z., Zhao, Y., and Shen, Z.: Chemical characterization and source apportionment of PM_{2.5} in Beijing: seasonal perspective, *Atmos. Chem. Phys.*, 13, 7053–7074, doi:10.5194/acp-13-7053-2013, 2013.
- Zhang, Y. M., Zhang, X. Y., Sun, J. Y., Hu, G. Y., Shen, X. J., Wang, Y. Q., Wang, T. T., Wang, D. Z., and Zhao, Y.: Chemical composition and mass size distribution of PM₁ at an elevated site in central east China, *Atmos. Chem. Phys.*, 14, 12237–12249, doi:10.5194/acp-14-12237-2014, 2014.
- Zheng, G. J., Duan, F. K., Su, H., Ma, Y. L., Cheng, Y., Zheng, B., Zhang, Q., Huang, T., Kimoto, T., Chang, D., Pöschl, U., Cheng, Y. F., and He, K. B.: Exploring the severe winter haze in Beijing: the impact of synoptic weather, regional transport and heterogeneous reactions, *Atmos. Chem. Phys.*, 15, 2969–2983, doi:10.5194/acp-15-2969-2015, 2015.
- Zheng, M., Salmon, L. G., Schauer, J. J., Zeng, L., Kiang, C. S., Zhang, Y., and Cass, G. R.: Seasonal trends in PM_{2.5} source contributions in Beijing, China, *Atmos. Environ.*, 39, 3967–3976, doi:10.1016/j.atmosenv.2005.03.036, 2005.

Aerosol composition, oxidative properties, and sources in Beijing

W. Q. Xu et al.

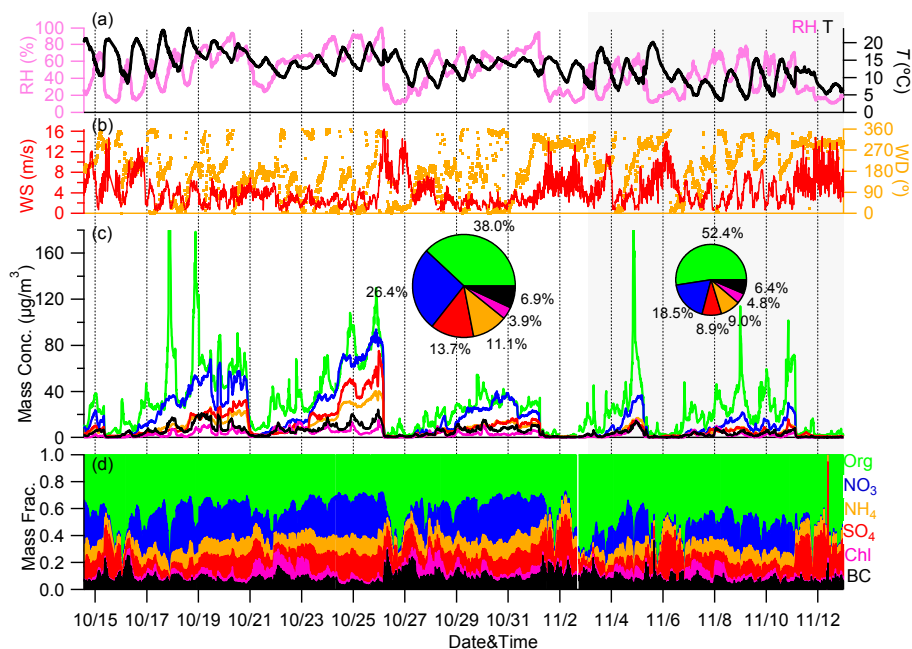


Figure 1. Time series of (a) relative humidity (RH), temperature (T), (b) wind direction (WD), wind speed (WS), (c) mass concentrations, and (d) mass fractions of chemical species in PM_{10} . The pie charts show the average chemical composition of PM_{10} measured before and during the Asia–Pacific Economic Cooperation (APEC) summit.

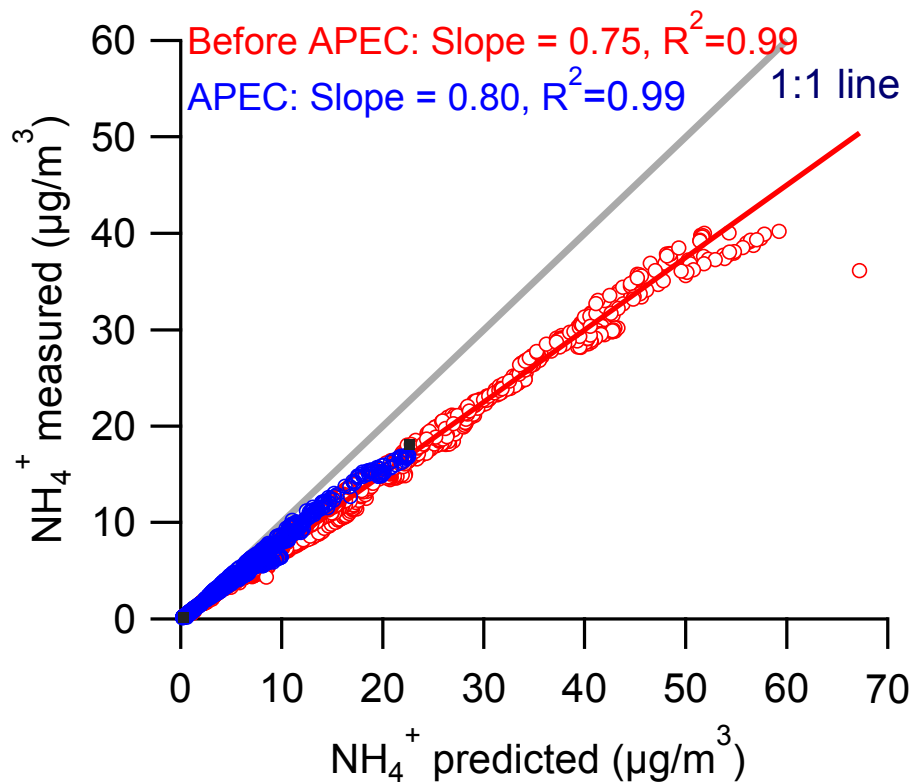


Figure 2. Correlation between predicted NH_4^+ and measured NH_4^+ recorded before and during the Asia–Pacific Economic Cooperation (APEC) summit.

Title Page

Abstract

Introduction

Conclusions

References

Tables

Figures

◀

▶

◀

▶

Back

Close

Full Screen / Esc

Printer-friendly Version

Interactive Discussion



Aerosol composition, oxidative properties, and sources in Beijing

W. Q. Xu et al.

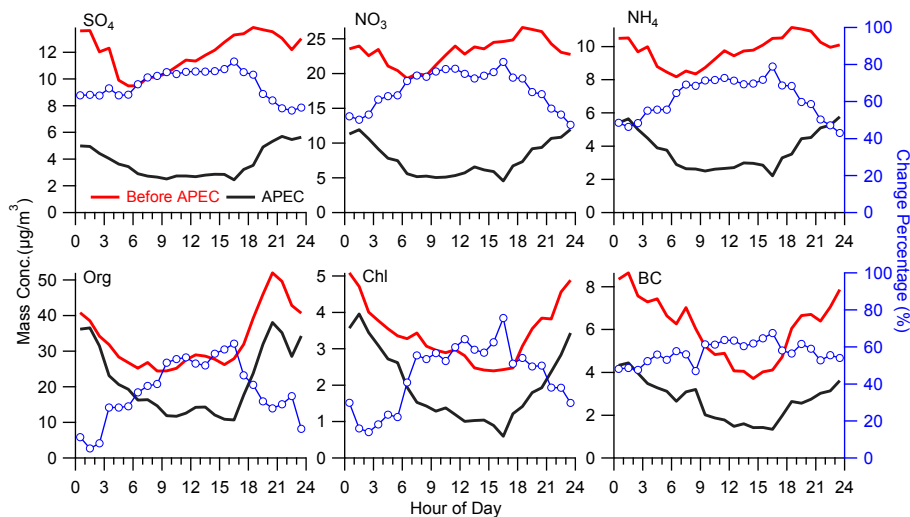


Figure 3. Diurnal profiles of the mass concentrations of PM_1 species measured before and during the Asia–Pacific Economic Cooperation (APEC) summit. Also shown are the changes in percentage of aerosol species occurring during APEC.

Title Page

Abstract

Introduction

Conclusions

References

Tables

Figures

◀

▶

◀

▶

Back

Close

Full Screen / Esc

Printer-friendly Version

Interactive Discussion



Aerosol composition, oxidative properties, and sources in Beijing

W. Q. Xu et al.

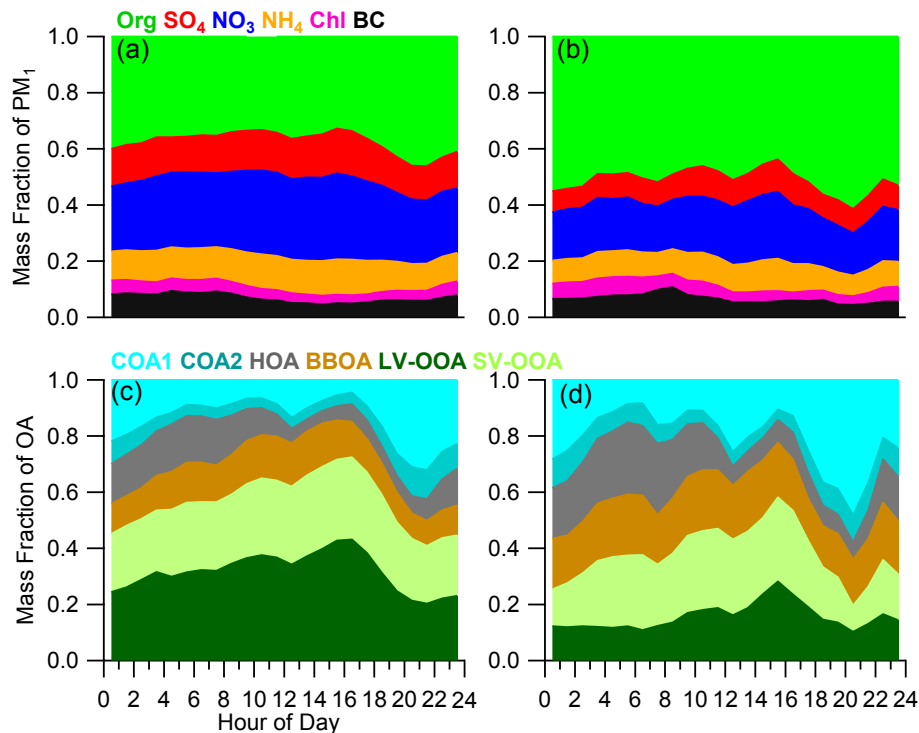


Figure 4. Diurnal evolution of the composition of PM_{10} and organic aerosols (OA) measured (a, c) before the Asia–Pacific Economic Cooperation summit (APEC) and (b, d) during APEC.

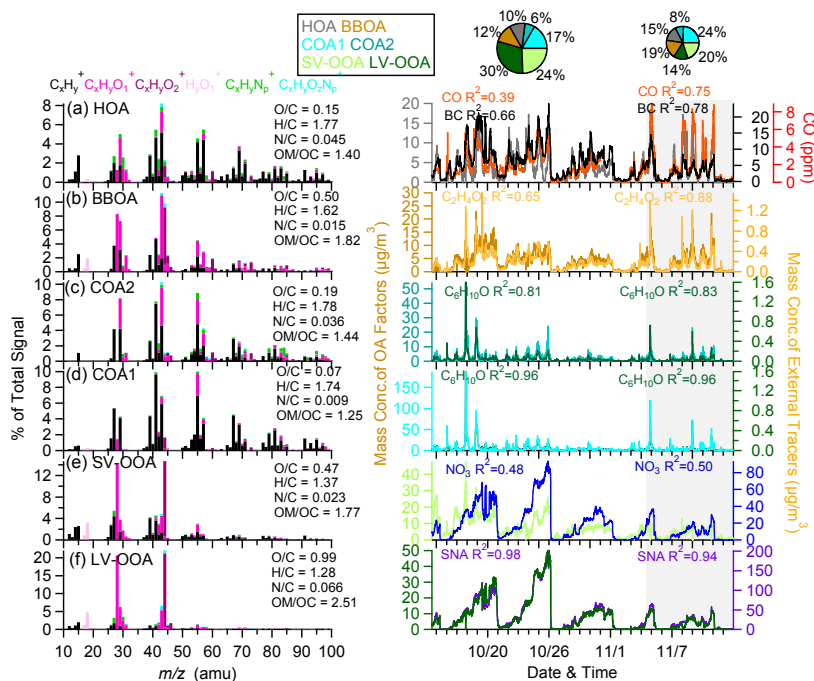


Figure 5. High-resolution mass spectra (HRMS; left panel) and time series (right panel) of six organic aerosols (OA) components **(a)** hydrocarbon-like aerosol (HOA), **(b)** biomass burning OA (BBOA), **(c)** cooking organic aerosol 2 (COA2), **(d)** COA1, **(e)** semi-volatile oxygenated OA (SV-OOA), and **(f)** low-volatility oxygenated OA (LV-OOA). Also shown in the right panel are the time series of external tracers including C₆H₁₀O⁺, C₂H₄O₂⁺, CO, black carbon (BC), nitrate and SNA (sulfate + nitrate + ammonium). The two pie charts show the average chemical composition of PM₁ measured before and during the Asia–Pacific Economic Cooperation (APEC) summit, respectively. The correlation coefficients between OA factors and external tracers measured before and during APEC are also shown in the figure.

Aerosol composition, oxidative properties, and sources in Beijing

W. Q. Xu et al.

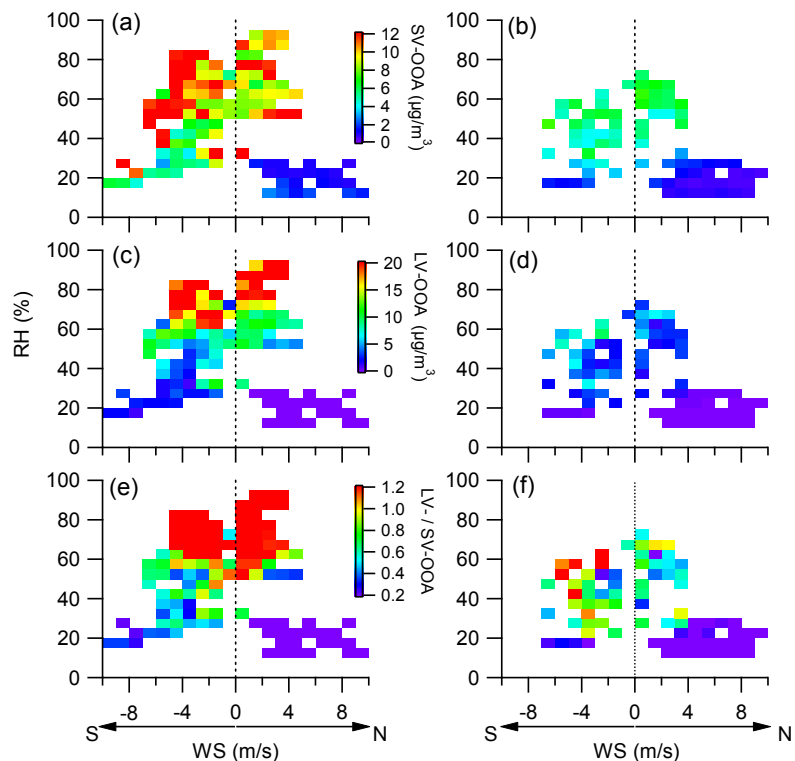


Figure 7. Relative humidity (RH) and wind dependence (WD) of **(a, b)** semi-volatile oxygenated organic aerosols (SV-OOA), **(c, d)** low-volatility oxygenated organic aerosols (LV-OOA), and **(e, f)** the ratio of LV-OOA/SV-OOA measured before (left panel) and during the Asia–Pacific Economic Cooperation (APEC) summit (right panel). S refers to the south ($90^\circ < \text{WD} < 270^\circ$), and N refers to the north ($0^\circ < \text{WD} < 90^\circ$ and $270^\circ < \text{WD} < 360^\circ$). Grids with points numbering less than five were excluded.

Title Page

Abstract

Introduction

Conclusions

References

Tables

Figures

◀

▶

◀

▶

Back

Close

Full Screen / Esc

Printer-friendly Version

Interactive Discussion



Aerosol composition, oxidative properties, and sources in Beijing

W. Q. Xu et al.

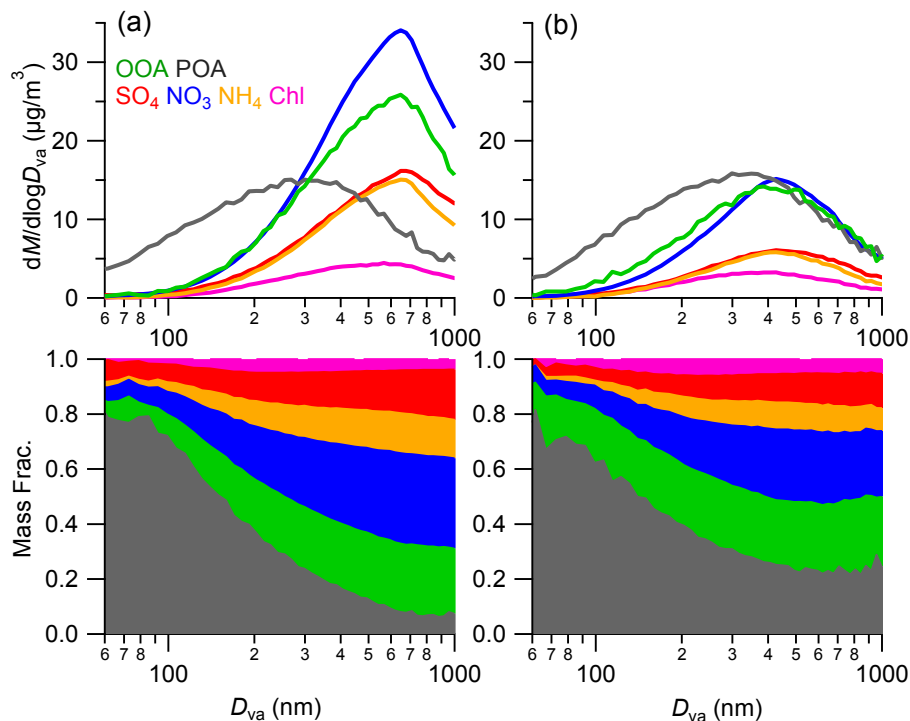


Figure 8. Average size distributions and fractions of NR-PM₁ species, primary organic aerosols (POA) and oxygenated organic aerosols (OOA) measured **(a)** before the Asia–Pacific Economic Cooperation (APEC) summit and **(b)** during APEC.

[Title Page](#)
[Abstract](#)
[Introduction](#)
[Conclusions](#)
[References](#)
[Tables](#)
[Figures](#)
[◀](#)
[▶](#)
[◀](#)
[▶](#)
[Back](#)
[Close](#)
[Full Screen / Esc](#)
[Printer-friendly Version](#)
[Interactive Discussion](#)

Aerosol composition,
oxidative properties,
and sources in
Beijing

W. Q. Xu et al.

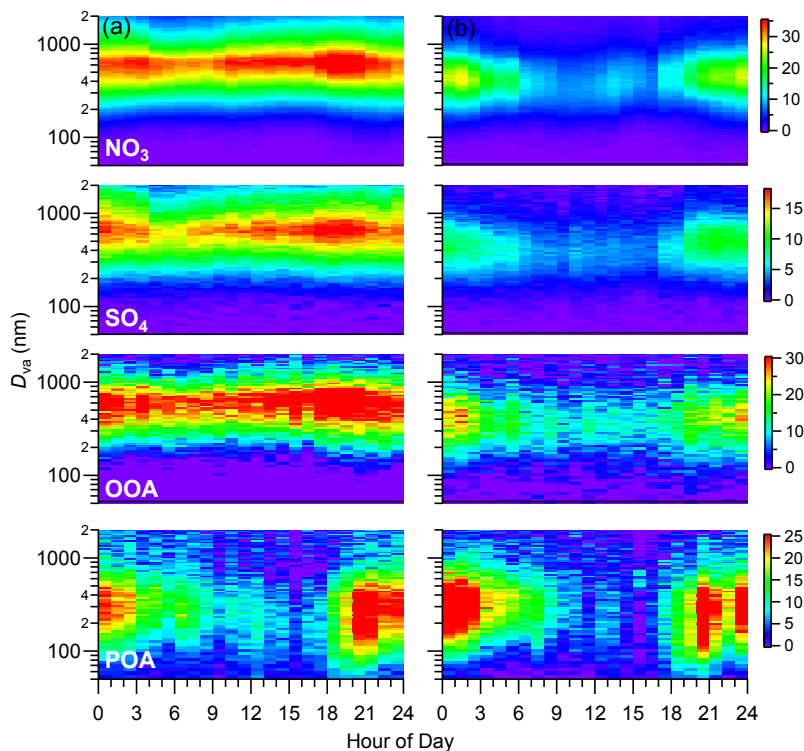


Figure 9. Diurnal evolution of the size distributions of NR-PM₁ species measured **(a)** before the Asia–Pacific Economic Cooperation (APEC) and **(b)** during APEC.

[Title Page](#)[Abstract](#)[Introduction](#)[Conclusions](#)[References](#)[Tables](#)[Figures](#)[◀](#)[▶](#)[◀](#)[▶](#)[Back](#)[Close](#)[Full Screen / Esc](#)[Printer-friendly Version](#)[Interactive Discussion](#)

Aerosol composition,
oxidative properties,
and sources in
Beijing

W. Q. Xu et al.

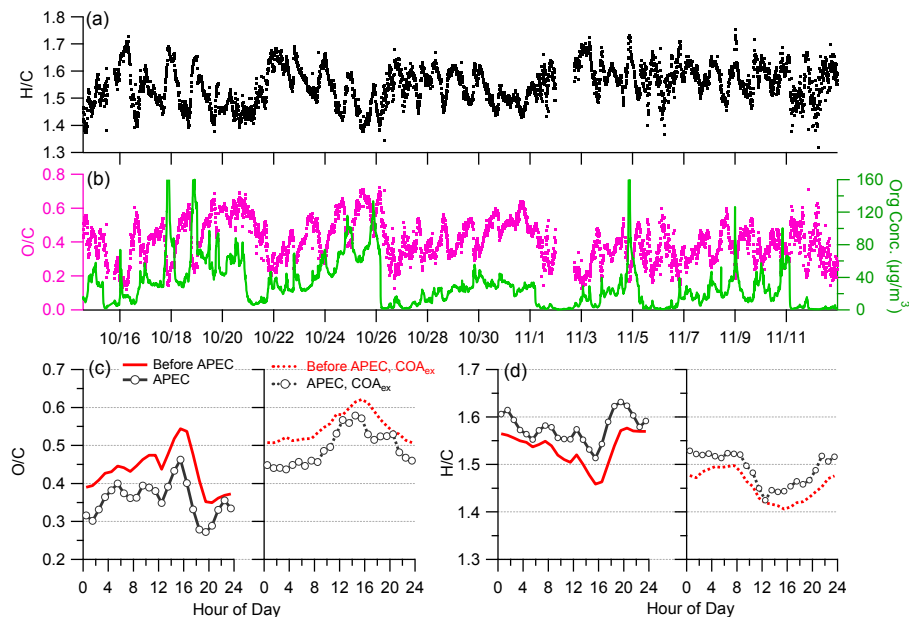


Figure 10. Time series of (a) H/C, (b) O/C, and organics, and diurnal variations of (c) O/C and (d) H/C. The dashed lines in (c) and (d) indicate the elemental ratios by excluding the contributions from cooking aerosols.

[Title Page](#)[Abstract](#)[Introduction](#)[Conclusions](#)[References](#)[Tables](#)[Figures](#)[◀](#)[▶](#)[◀](#)[▶](#)[Back](#)[Close](#)[Full Screen / Esc](#)[Printer-friendly Version](#)[Interactive Discussion](#)

Aerosol composition,
oxidative properties,
and sources in
Beijing

W. Q. Xu et al.

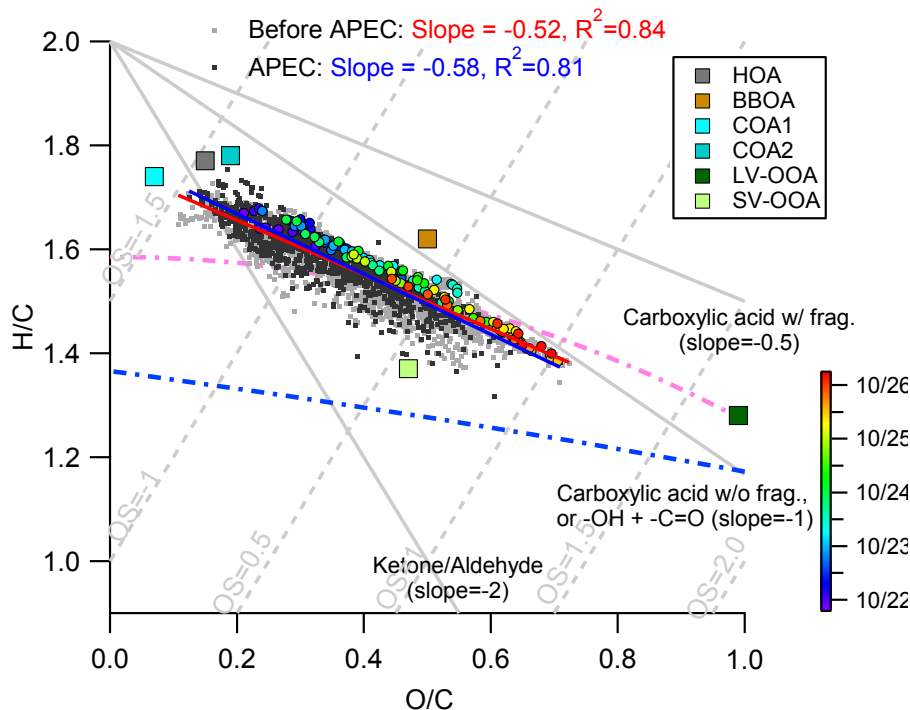


Figure 11. Van Krevelen diagram of H/C versus O/C. The dashed lines indicate changes in H/C against O/C due to the addition of specific functional groups to aliphatic carbon (Heald et al., 2010). The pink and blue lines are derived from the right and left lines in the triangle plot of positive matrix factors (PMF) determined from 43 sites in the Northern Hemisphere (Ng et al., 2011). The color-coded H/C versus O/C refers to the data measured during the severe haze episode shown in Fig. 13.

**Aerosol composition,
oxidative properties,
and sources in
Beijing**

W. Q. Xu et al.

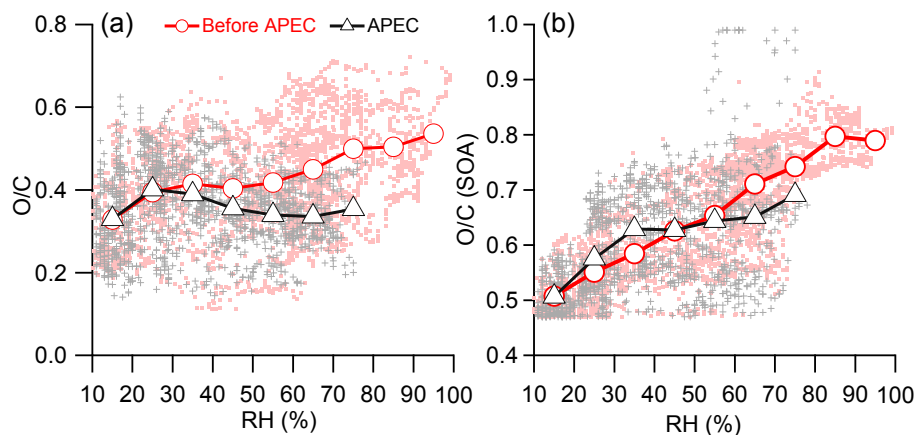


Figure 12. Variations in (a) O/C and (b) O/C of secondary organic aerosols (SOA) as a function of relative humidity (RH) measured (a) before the Asia–Pacific Economic Cooperation (APEC) summit and (b) during APEC. The data are also binned according to RH with increments of 10%.

[Title Page](#)[Abstract](#)[Introduction](#)[Conclusions](#)[References](#)[Tables](#)[Figures](#)[◀](#)[▶](#)[◀](#)[▶](#)[Back](#)[Close](#)[Full Screen / Esc](#)[Printer-friendly Version](#)[Interactive Discussion](#)

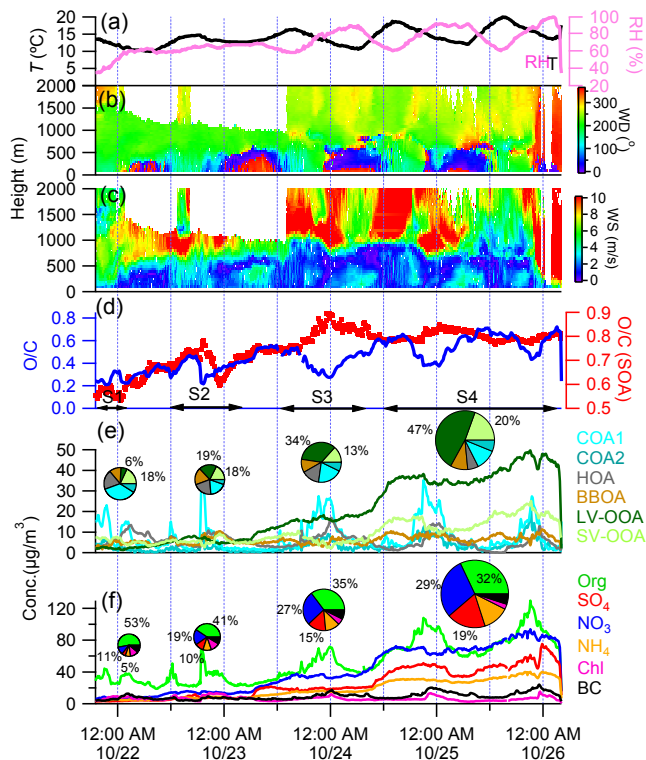


Figure 13. Evolution of meteorological variables including (a–c) relative humidity (RH), temperature (T), and vertical profiles of wind direction (WD) and wind speed (WS); (d) O/C and O/C of secondary organic aerosols (SOA); (e) organic aerosol (OA) factors; and (f) PM_{10} species. The pie charts show the average chemical composition of PM_{10} and OA for each stage. The numbers on the pie charts show the contributions of (e) semi-volatile oxygenated organic aerosols (SV-OOA) and low-volatility oxygenated organic aerosols (LV-OOA) and (f) organics, nitrate, and sulfate.

Aerosol composition, oxidative properties, and sources in Beijing

W. Q. Xu et al.

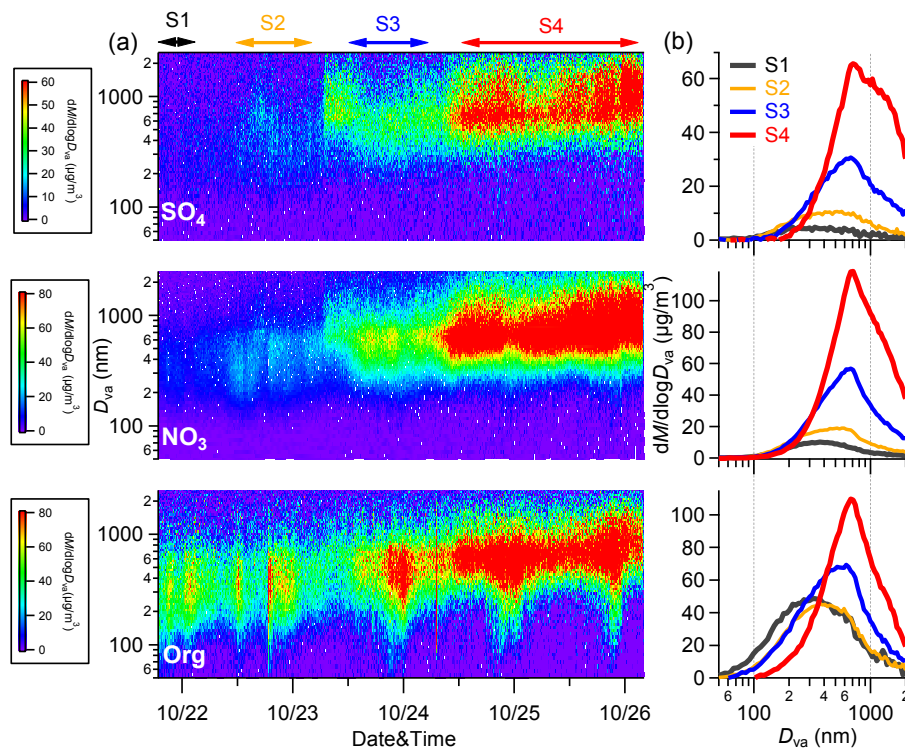


Figure 14. (a) Evolution of size distributions of sulfate, nitrate, and organics. (b) Average size distributions of these three species for each stage.